ADAM KOTOWSKI · KRZYSZTOF STEFANIAK RALF-DIETRICH KAHLKE

A RHINOCEROTID SKULL FROM THE EARLY PLEISTOCENE SITE OF UNTERMASSFELD

Abstract

The fossil rhinocerotid material from Untermassfeld represents at least 36 individuals. The total material of more than 1,000 finds, however, contains only one single skull of an adult animal, which is described and discussed here. At the time of its embedment in a fluviatile erosion channel leeside of a clastic mudflow fan, both horns had already been lost. Confirmed by morphological traits and dimensions, the skull has been assigned to a female individual of *Stephanorhinus hundsheimensis* with especially small horns.
In rhinocerotid skulls, the ratio of the length of the nasal bones to the distance between the narial notch and the rostral rim of the orbit, combined with the degree of ossification of the nasal septum, reveals five types of adaptation that have evolved to bear the respective mass of the horns. *S. hundsheimensis* is grouped together with *S. hemitoechus* and *S. kirchbergensis,* although the horns of the former might have been a little lighter than those of the latter. The rhinocerotid palaeo-population from Untermassfeld belongs to the older representatives of *S. hundsheimensis* in the western Palaearctic.

1. Introduction

The first discovery of fossil rhinocerotid remains at Untermassfeld was published by H.-D. Kahlke (1980; 1982). In fact, it was the discovery of a fragment of rhinocerotid tooth, one of the earliest finds recovered from the site, which led to its immediate inspection in January 1978 (pers. comm. H.-D. K. to R.-D. K.) and the subsequent establishment of a protected area for future palaeontological excavations (R.-D. Kahlke 1997). As part of the first monographic study, the hitherto available rhinocerotid material was described and discussed in detail by H.-D. Kahlke (2001). Based on Kretzoi (1942), and using a morphometrically-speaking broad species terminology, he assigned the Untermassfeld rhinocerotid population to *Stephanorhinus etruscus* (Falconer 1859).
At the time of the first study the Untermassfeld rhinocerotid material comprised 651 specimens, including 310 isolated skeletal elements, 56 elements from anatomically connected units, and 285 elements from reconstructed skeletal units (R.-D. Kahlke 2001, 953ff., Figs. 11, 13–18, Tab. 2) Based on these finds, a minimum number (MNI) of 29 individuals, comprising 13 juveniles/subadults and 16 adults, was determined (R.-D. Kahlke 2001; 2006). The only largely intact find from a rhinocerotid skull was the calvarium of

a juvenile individual [IQW 1985/20503 (Mei. 20023)] with the D1-D4 and erupting M1 on both sides (H.-D. Kahlke 2001, 502 ff., fig. 1, pls. 79–80). This find was excavated in 1984 from grid square Q 532, 0.65 m below site 0-level (for documentation see Kahlke in volume 5). Prior to this, skulls of adult individuals, or even isolated permanent teeth of the upper dentition, had not been recovered from the site.
In the meantime (as of 1 May 2019), 1,065 rhinocerotid finds of at least 36 individuals, namely 13 juveniles/subadults and 23 adults, have now been recovered from the site including the almost complete skull of an adult individual, still preserving both tooth rows. This skull was excavated on August 1, 2007 and its final preparation and conservation was reported with much fanfare by the local press (Wagner 2008a; 2008b; 2008c). Its find-position, state of preservation and morphology are described and discussed below Following Fortelius et al. (1993), Lacombat (2005; 2007), and Kahlke et al. (2011), we have assigned the Untermassfeld rhinocerotid population to *Stephanorhinus hundsheimensis* (Toula, 1902), while acknowledging that the phylogenetic position of this species has not yet been unequivocally clarified.

2. Depositional environment, taphonomy and diagenetic processes

The skull IQW 2009/30270 (Mei. 29432) of a fully adult *S. hundsheimensis* (**Fig. 1**) was retrieved from the lower part of Upper Fluviatile Sands [UFS(I)]. It was deposited immediately after the peak of a strong flood in an erosion channel (R.-D. Kahlke 2001; 2006; Kahlke et al. in this volume). The fossil was recovered from grid squares Q 24 and 29, 2.61–2.50 m below site 0-level (Kahlke 2007a, fig. 3; in volume 5, Fig. 9, Foldout III). It was found as an isolated skeletal element, with no evidence of individually related finds in its vicinity. The longitudinal axis of the rhinoceros skull was oriented parallel to the flow direction of the river, i.e. in a SE-NW direction. The skull became embedded in a large mammal bone accumulation that had formed leeward of a clastic mudflow fan as a result of the flow regime of the river (CMF; detailed description Kahlke in volume 5). It was embedded capsized, with its ventral surface facing upwards (corresponding to **Fig. 1d**) and, therefore, the presence of the nasal and frontal horns on the skull during the embedment process can be ruled out. The skeletal elements accumulated in the fossiliferous UFS(I) are largely items that can be readily transported by flowing water; thus it is clear that the absence of the horns was a precondition in order for the rhinoceros skull to be washed into the area of the site. Obstructive skeletal elements or anatomically connected units are rare or completely absent in the Untermassfeld fossil assemblage (R.-D. Kahlke 2001, 959 ff.; 2006, 55 f.)
The rhinocerotid skull shows clear bite and gnaw marks caused by *Pachycrocuta brevirostris* (**Fig. 1**). These gnaw marks are found on both of the occipital condyles, the occiput, and the bony part of the nasal septum. In addition, the right facial skeleton, especially the zygomatic arch and the anterior margins of the nasal bone, also displays significant damage by hyaena. The rhinoceros head was exposed to hyaena ravaging apparently while it was lying on its left side. The evidence indicates that the occiput and nasal tip were freely accessible to the predators. That the horns were still attached to the skull at this time cannot be ruled out, but they might have been loosened due to the destruction of adjacent tissue during the gnawing of the nasal region by hyaena. Rhinocerotid horns are known to fall off from decomposing carcasses with relatively little physical effort (Garutt 1998); hence, the loss of the horns happened, at the latest, during the subsequent transport of the (?partial) cadaver by water. Since the fossil skull shows no signs of weathering, insolation, rolling or abrasion by sediment particles, it was presumably not transported over long distances, but quickly deposited in UFS(I).
Modifications of the bone surfaces by plant root etching are common in the Untermassfeld vertebrate assemblage. They point to rapid post-depositional overgrowth of the well-manured fossiliferous sands by a

plant cover (R.-D. Kahlke 2001, 976; 2006, 81). The etching patterns are particularly pronounced on the ventral side of the nasals (which were facing upward in their find-position), on the bony nasal septum, and even on the occlusal surface of the right M^1. To a lesser extent, they are also found on both sides as well as on the dorsal face of the skull. There are some etching traces on the frontal bone, within the rugose attachment area of the horn, which prove that it was separated from the skull or destroyed before the time of root penetration.
The preservation state of the teeth and bone parts of the skull is generally good due to the presence of carbonate in the embedding sands (Ellenberg and Kahlke 1997, 45). The plastic deformation of the skull is a result of neotectonic movements that led to a dipping of the sediments towards the southwest (Ellenberg and Kahlke 1997, 54 ff.). The increasing dip angle (up to 130/20 SW) caused a pronounced compression of the UFS(I) and of its fossil content.

3. Description

Specimen IQW 2009/30270 (Mei. 29432) is an almost complete skull with complete dentition (P^2-M^3 sin. et dex.). In accordance with the overall character of the fossiliferous site (see section 2.), its state of preservation is generally good (**Fig. 1**). The cranial and dental measurements were taken according to a modified method proposed by Guérin (1980) and Van der Made (2010) with additions and altered numbering. Abbreviations proposed by the latter are applied here. All measurements are given in **Fig. 2**.

3.1. Cranial morphology

The skull lacks a part of the right zygomatic arch, namely the zygomatic process of the squamous part of the temporal bone, up to half the length of the zygomatico-temporal suture (see section 2.). The orbits are situated halfway along the length of the skull (**Fig. 1a–b**). Caudally, the most protruding parts of the skull are the occipital condyles and external occipital tuberosity (**Fig. 1a–b, d**), thus the occiput is perpendicular to the base of the skull.
The right side of the skull is deformed (**Fig. 1a, c**), with some of the bones having moved medially during the deformation process. Maxillary and zygomatic bones were moved without suffering any deformation, whereas the medial part of the orbit, the pterygopalatine fossa and temporal fossa are distorted. The whole area of the lacrimal bone with the nasolacrimal, maxillolacrimal and zygomatico-lacrimal sutures is dented. The praeorbital process has become separated and is intact, but the supraorbital process of the frontal bone is bent and tucked into the orbit. The right dental arch is unaltered. The hamulus of the right pterygoid bone is not preserved. Due to deformation the orbital fissure is not visible. In the right temporal area, the parietal bone and temporal squama are bent parallel to the temporal line. The area of the external acoustic meatus is intact and the ear canal is completely preserved. The peripheral parts of the retroarticular process and paracondylaris process are missing.
Both nasal bones are complete (**Fig. 1a–c**). The nasofrontal and the internasal sutures are completely fused. The internasal suture does not reach the rostral tip of the nasals, forming a small, around 25 mm-long fissure. In dorsal view, the nasal bones have a triangular outline, with the widest point at level of the nasomaxillar sutures. Both horns were probably relatively small. The base of the anterior horn is roughly oval or triangular-shaped, and measures approximately 168 × 120 mm. The basal rugosity of the anterior horn is oval and has a width around 1/3 the width of the nasals. The protuberance at the centre of it is situated

Fig. 1 *Stephanorhinus hundsheimensis* (Toula), Untermassfeld. – **a–d** Skull of an adult female individual IQW 2009/30270 (Mei. 29432), right and left lateral, dorsal, ventral views. – Scale: 50 mm.

95 mm from the tip of the nasals. Generally, the surface of the nasals is only mildly rugose, and not so much cauliflower-shaped as it is in the woolly rhinoceros. The rostral part of the protuberance and the lateral margins, near their greatest width, are the most rugose surfaces of the nasals. The nasal septum is ossified in its rostral part, at the base of the anterior horn; its length is roughly 1/3 the distance between the tip of the nose and the nasoincisive notch.

The praemaxillary bones are very narrow, around half the width of the nasals, and have an acute triangular outline in dorsal view (**Fig. 1d**). The free margins of the praemaxillary bones have acute edges. The rostral tips of the praemaxillaries are separated by a broad interincisive fissure which extends for half the length of the palate, from the tip of the praemaxillary bones to the P^2. Because of this long fissure, a part of the nasal septum is not supported. The bone of the nasal septum is fused with the praemaxillary bones for only half its length (**Fig. 1a–b**). The general proportions of the nasal and praemaxillary bones, the degree of ossification of the septum, together with the slight rugosity of the horn base indicate that the anterior horn was relatively small and light.

The surface of the frontal bone is flat and smooth, in all but the small base of the posterior horn, which is located near the nasofrontal sutures (**Fig. 1a–c**). The base of the posterior horn is smaller than the anterior one. It includes two small, slightly rugose areas (**Fig. 1c**), and its outline measures 95 × 80 mm. At its centre there is a single nutritive foramen with a diameter of 4 mm. The horn base does not extend caudally farther than half the length of the orbits. The whole structure is located between the nasoincisive notch and the supraorbital process. The bases of the two horns are clearly separated. At its greatest width, the forehead is twice as broad as the widest part of the nose, which is the widest point of the base of the anterior horn. The forehead curves smoothly round into the temporal fossa.

The left facial area of the skull is well-preserved (**Fig. 1b–c**). The orbital rim is not very raised and prominent temporal lines, each in the shape of two parallel ridges, run from behind the orbits backwards (**Fig. 1c**). The area of insertion of the orbital ligament, at the caudal margin of the left orbit, is not very clear The infraorbital foramina are visible. The facial tuberosities are distinct and start on lines joining the praeorbital process and the rostral edge of the M^2, before seamlessly turning into the temporal processes of zygomatic bones. The praemaxillo-maxillary, zygomatico-maxillary and fronto-maxillary sutures are fused, whereas the zygomatico-lacrimal and zygomatico-temporal sutures are not. The praeorbital processes are single and slender On the left side, the insertion of the orbital ligament is distinct and located on the zygomatico-lacrimal suture. There is a single, elongated, caudal lacrimal foramen. Above it, at the height of the praeorbital process, is a shallow trochlear fovea (**Fig. 1b**).

The left parietal bone is not so strongly constricted as it is in the woolly rhinoceros. The temporal lines become more distinct and are closer spaced to each other moving towards the skull roof. The medial ones, at the height of the external acoustic meatus, converge in the sagittal plane, creating a very delicate sagittal crest and then disappear before reaching the occipital crest (**Fig. 1c**).

The temporal regions are severely damaged, mostly in the area of the occipital crest (**Fig. 1a–c**). The articular facet of the left articular tubercule lies perpendicularly to the long axis of the skull along most of its length. Only in its medial part it protrudes caudally with an around 45° inclination. The left articular tubercule is slightly convex, whereas the right one is laterally broken (**Fig. 1d**).

The occiput is partly damaged, especially the squama, from the external occipital protuberance to the occipital crest (**Fig. 1a–c**). The lateral parts and the base are better preserved. The external occipital tuberosity is strongly convex and approximately the size of each occipital condyle. The occipital condyles are trapezoid. Their long axes are not horizontal, but oblique, and are situated along the line joining the external acoustic meatus with the foramen magnum. The outline of the occipital crest is damaged and cannot be described.

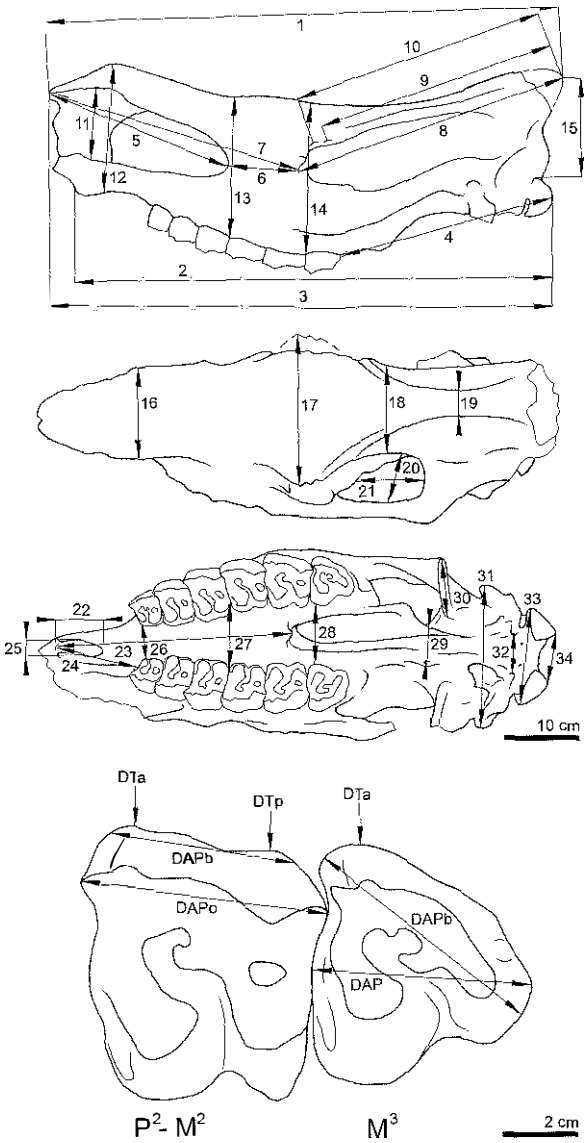

Fig. 2 Cranial measurements. – 1 Dorsal length of the skull from the tip of the nasals to the occipital crest. – 2 Ventral length of the skull from the tip of the praemaxillaries to the caudal end of the occipital condyles. – 3 Total length of the skull from the tip of the nasals to the caudal end of the occipital condyles. – 4 Distance between M^3 and the caudal end of the occipital condyle. – 5 Distance from the tip of the nasals to the caudal-most point of the naso-incisive notch. – 6 Distance from the caudal-most point of the naso-incisive notch to the rostral margin of the orbit. – 7 Distance from the tip of the nasals to the rostral margin of the orbit. – 8 Distance from the rostral margin of the orbit to the occipital crest. – 9 Distance from the supraorbital process to the occipital crest. – 10 Distance from the postorbital process to the occipital crest. – 11 Greatest height of the nasal aperture. – 12 Height of the skull in the nasal region. – 13 Height of the skull above the anterior border of M^1. – 14 Height of the skull above the anterior border of M^3. – 15 Height of the squamous part of the occiput from the dorsal border of the foramen magnum to the occipital crest. – 16 Width of the nasals. – 17 Greatest width of the forehead between the supraorbital processes. – 18 Smallest width of the calvarium. – 19 Smallest distance between the temporal crests. – 20 Width of the temporal fossa. – 21 Length of the temporal fossa. – 22 Length of the interincisive fissure. – 23 Greatest length of the palate from the tip of praemaxillaries to the caudal nasal spine. – 24 Length of the free border of praemaxillary bone. – 25 Width of the interincisive fissure. – 26 Width of the palate between the P^2. – 27 Width of the palate between the P^4/M^1 borders. – 28 Width of the palate between the M^3. – 29 Distance between the caudal alar foramina. – 30 Width of the articular tubercule facet of the temporal bone. – 31 Greatest width of the occiput between the mastoid apophyses. – 32 Distance between the hypoglossal foramina. – 33 Width between the lateral margins of the occipital condyles. – 34 Width between the medial margins of the occipital condyles. – 35 Width of the retroarticular process, transverse diameter (not shown). – 36 Length of the retroarticular process, rostro-caudal diameter (not shown). – 37 Greatest width of the piriform aperture (not shown). – 38 Width of the skull at the praeorbital foramina (not shown). – 39 Thickness of the bony part of the nasal septum (not shown). – 40 Width of the foramen magnum (not shown).
Measurements of the P^2-M^2. – DAPo Occlusal antero-posterior dimension on the buccal side. – DAPb Basal antero-posterior dimension on the buccal side at the height of the border between the roots and the crown. – DTa Anterior transverse dimension at the widest point of the rostral part of the crown. – DTp Posterior transverse dimension at the widest point of the rostral part of the crown.
Measurements of the M^3. – DAP Antero-posterior dimension measured perpendicularly to a line contiguous to the rostral border of the tooth. – DAPb Antero-posterior dimension, i.e. the greatest length of the buccal side of the tooth. – DTa Anterior transverse dimension, analogical to DTa in the P^2-M^3.

The alveolar margins of the maxillar bones are relatively high, thus the palate is domed transversely (**Fig. 1d**). The whole palate, from the tips of the praemaxillary bones to the perpendicular flange of the palatine bones, is roughly arrow-head-shaped. The palate is smooth with no rugae. The medial palatal suture is strongly damaged along most of its length, except the caudal-most part, where it is hardly visible. The palato-maxillary sutures are fused. The medial palatal suture of the horizontal plates of the maxillary bones is not fused to the same degree, and appears as a delicate crest which ends aborally into a distinct, caudal nasal spine. The right greater palatine foramen is located at the height of the nasal spine. The minor palatine foramina are distinct and located at the height of the anterior edge of M^3.

Distance		Distance		Distance		Distance	
1	(628)	11	95	21	(135)	31	191
2	635	12	175	22	61	32	56
3	661	13	222	23	276	33	130
4	292	14	242	24	97	34	61
5	242	15	144	25	18	35	88
6	99	16	121	26	47	36	13
7	316	17	(234)	27	72	37 (sin)	33
8	(351)	18	(111)	28	67	37 (dex.)	33
9	(342)	19	35	29	36	38	110
10	(313)	20	(80)	30	91	39	16
						39 (dex.)	23
						40	45

Table 1 Cranial measurements of the *Stephanorhinus hundsheimensis* (Toula) skull IQW 2009/30 270 (Mei. 29432). Measured distances are illustrated in Fig. 2. Measures in mm.

The inner wall of the orbit and the pterygo-palatine fossa are the most damaged area of the left side of the skull; the deformation caused the closure of the fossa. The best-preserved parts are the fragments of the perpendicular flange of the palatine bone, part of the sphenoid, and the pterygoid bone, whose hamulus is not preserved (**Fig. 1d**). The palato-maxillar and the palato-sphenoidal sutures are the clearest of the whole skull. A distinct foramen in this area, 9 mm across, seems to be the optic canal, but because of the strong deformation this remains unclear.

The vomer is present on the whole length of the soft palate and is severely damaged. In contrast to the rest of the skull, the right side of its base is better preserved. The praesphenoid and basisphenoid bones are completely fused. On the right of them the caudal alar foramen is preserved, whereas on the left only part of its medial margin remains (**Fig. 1d**)

The muscular tubercles on the basisphenoid bone are not very prominent. The lacerum foramina on both sides are impossible to describe because of the presence of bone fragments within them. In this area only the styloid processes are visible (**Fig. 1d**). The canals of the hypoglossal nerves are distinct and deep, but the left ones are mostly obstructed by the lateral part of the occiput, which was displaced into this area. The peripheral parts of the retroaticular and paracondylar processes are not preserved, and therefore their overall shape is unclear.

The cranial measurements (**Fig. 2**) are listed in **Table 1**.

3.2. Dentition

Both tooth rows are complete and are little damaged (**Fig. 1d**) Individual teeth on both sides of the skull are described together Measurements are given in **Table 2**.

Second upper premolars (P^2): The buccal edge is convex; the parastyle points slightly out in a rostral direction and the paracone fold is mildly marked. The caudal edge of the ectoloph does not extend outside the outline of the occlusal surface. The protocone is drop-shaped, and the hypocone widens peripherally in a

caudal direction. The praefossette is closed by the protocone and the hypocone. The postfossette is also completely closed by the fused hypocone and the ectoloph. The mediofossette is closed in the left tooth (and is unobservable in the right). There is no antecrochet. The cingulum is well-developed and surrounds the whole protocone and the lingual valley The enamel is almost smooth on the lingual side, whereas on the buccal side it is smooth near the occlusal surface and crenulated closer to the roots. Both right and left teeth are missing some parts of the enamel in the hypocone area.

Third upper premolars (P^3): The buccal edge is mildly convex but to a lesser extent than that observed in the P^2. The parastyle protrudes in a rostrobuccal direction. The fold of the paracone is delicately formed. The protocone is drop-shaped, the hypocone widens peripherally in a caudal direction. Praefossette and postfossette are completely closed. The mediofossette is gently marked by a delicate crochet. An antecrochet does not exist. The cingulum is strongly developed, starting under the protoloph and surrounding the protocone. It is only slightly visible at the lingual valley and fuses with the occlusal edge of the hypocone. The enamel is developed similar to that observed in the P^2.

Fourth upper premolars (P^4): The buccal side is rather straight. The parastyle is very prominent and points in a rostrolateral direction, similar to that observed in the preceding premolars. The paracone fold is delicate but present. The caudal margin of the ectoloph is slightly bent in a buccal direction. The shape of the protocone is similar, whereas the hypocone is oval. The praefossette and postfossette are closed. The mediofossette is slightly marked in the right tooth by the presence of a small crest, which is absent in the left tooth. An antecrochet is absent. In the right tooth, there is a single crest. A cingulum appears on the protoloph, disappears at the height of the lingual edge of the protocone, and then reappears near the lingual valley. As in P^3 it fuses with the occlusal surface of the hypocone. The enamel on the lingual side is generally smooth, except in the lingual valley where it is slightly crenulated. On the buccal side, the upper half of the crown is smooth, becoming gradually crenulated towards the root.

First upper molars (M^1): The buccal outline is sinusoid. The parastyle protrudes rostrally. The caudal edge of the ectoloph protrudes slightly in a caudal direction. The protocone is rectangular with a small constriction, whereas the hypocone is U-shaped. The praefossette is open and fused with the lingual valley, the postfossette remains closed. The mediofossette is clearly marked by a rounded lobe of the metaloph (instead of a crochet, but with a very small surface). The cingulum is well-developed between protoloph and protocone. In the left tooth there is also a tubercule-like structure. In both teeth there is a structure resembling a small valley between the protoloph and the protocone that is closed by the cingulum. In the other parts of the teeth the cingulum is absent. The enamel resembles P^2 and P^3.

Second upper molars (M^2): The parastyle and the protocone fold are well-developed. There is a slight protocone constriction, although even smaller than that observed in the M^1. The outline of the buccal side is sinusoid. The caudal edge of the ectoloph has a distinct caudolateral protrusion in the left tooth only. The protocone is more of a triangular shape. The hypocone is rounded in the right tooth, whereas it is U- to V-shaped in that on the left. The praefossette and mediofossette are in the shape of a question mark and both are open. An evident crochet and a small crest at the height of the paracone fold appear in the left tooth. In the right the crochet is doubled, lingually more lobe-like, with a small crest-like structure on its buccal side. The cingulum is developed as in the M^1. The lingual enamel is smooth on the protocone but crenulated on the hypocone. The buccal side is completely crenulated.

Third upper molars (M^3) Both teeth are in the shape of a regular triangle. The ectometaloph is slightly arched. The parastyle and paracone fold are the most pronounced of the whole dentition. The protocone is rounded, yet open and limited by. The praefossette is open and a postfossette does not exist. The mediofossette is distinct a wide, hook-like crochet and a single, small crest at the height of the paracone fold. Both cingulum and enamel are developed similar to that observed in the M^2.

Tooth	Measurement			
	DAPo	DAPb	DTa	DTp
P^2 sin.		30.4	37.5	42
P^2 dex.	35.5	31.4	38.9	
P^3 sin.	40	37.2	52.6	49.4
P^3 dex.	39.4	36.7	51.1	49.3
P^4 sin.	44.9	41	(61)	(56 9)
P^4 dex.	44.4	42.1	58.2	55.3
M^1 sin.	47.9	49	(58.3)	(53 7)
M^1 dex.	49.5	47.3	57.3	53.7
M^2 sin.	54.8	50.7	(61 5)	(52 5)
M^2 dex.	49.5	47.3	57.3	53.6
	DAP	DAPb	DTa	
M^3 sin.	47.7	56.3	53.9	
M^3 dex.	45.7	57.5	54.1	

Table 2 Dental measurements of the *Stephanorhinus hundsheimensis* (Toula) skull IQW 2009/30270 (Mei. 29432). Measured distances are illustrated in **Fig. 2**. Measures in mm.

4. Morphometric comparison

One of the most striking diagnostic features separating the skulls of *S. hundsheimensis* from those of *S. etruscus* and of stratigraphically younger members of the genus is the shape of the snout area. *S. hundsheimensis* has elongated nasals and frontals (Lacombat 2005; 2007). According to Guérin (1980), Fortelius et al. (1993) and Schreiber (1999; 2005), the caudal margin of the nasoincisive notch is situated above the P^4/M^1 and the rostral margin of the orbit lies above the M^2. In *S. kirchbergensis,* the caudal margin of the nasoincisive notch is located above the P^3 or P^3/P^4 and the rostral margin of the orbit above the M^1/M^2 or M^2. In *S. etruscus,* the caudal margin of the nasoincisive notch is situated more rostrally, above the P^4, and the rostral margin of the orbit is situated a little farther caudally, above the M^2. In IQW 2009/30270 (Mei. 29432) the caudal margin of the nasoincisive notch lies above the rear half of the P^4 and the rostral margin of the orbit above the border of the M^1 and M^2 (**Fig. 1a–b**), which are features suggestive of *S. hundsheimensis.*

The lambdoidal crest of the Hundsheim rhinoceros is less elongated caudally than in *S. etruscus* and *S. kirchbergensis.* In IQW 2009/30270 (Mei. 29432) this feature is unclear due to the damaged state of the specimen. However, the angle between the base and the occiput of the skull suggests that the lambdoidal crest was shorter than in *S. etruscus* and *S kirchbergensis,* and thus like that of *S. hundsheimensis.*

According to Lacombat (2005; 2006b; 2007), both the M^1 and M^2 of the brachyodont *S etruscus* show a characteristic protocone constriction. In the molars of this species there is a single, well-developed crochet, a crest that is not always present, and a non-protruding protocone fold. In *S. hundsheimensis* the teeth are also brachyodont, without cementum. A crest is commonly present in the premolars, as well as the crochet. The protocone constriction is absent in the premolars, and rarely present in the molars. Compared to *S. etruscus* the protocone fold is strongly protruding.

Later representatives of the genus, i.e. *S. hemitoechus* and *S. kirchbergensis,* have more hypsodont teeth. In *S. hemitoechus* the premolar row is shortened, the protocone fold is strongly protruding, and the crest, antecrochet, and protocone constriction are not very common. In *S. kirchbergensis* a multiple crochet is visible in the premolars, as well as the protocone constriction and a narrower protocone fold in the molars.

In IQW 2009/30270 (Mei. 29432) the teeth are semi-hypsodont. The premolars show neither cementum nor protocone constrictions, whereas a mild constriction is visible in the M^1 and even less clearly marked on the M^2. The protocone folds in general are strongly protruding. The crochets are single (in all the teeth but the right M^2) and antecrochets are absent. There are single crests on the right P^4 and both of the M^3 (**Fig. 1d**). All these features are suggestive of *S. hundsheimensis* rather than of other *Stephanorhinus* species.

IQW 2009/30270 (Mei 29432) was compared with rhinocerotid skulls from key fossiliferous sites as well as with all extant species. Comparative data were collected from the following material:

- *S. hundsheimensis* from Hundsheim (Schreiber 1999; 2005), Mauer (Schreiber 1999; 2005), Isernia la Pineta (University of Ferrara, own measurements), Cagnes, Biarritz, Daxlanden, Pogi, Mosbach, Darmstadt, Bammental, and Cromer Forest Bed (Guérin 1980);
- *S. jeanvireti* from Vialette (Guérin 1980);
- *S. etruscus* from the Upper Valdarno including Olivola (Museum of Geology and Palaeontology, University of Florence, own measurements), Barberino (Museum of Palaeontology and Geology Bologna, own measurements), Florence (Museum of Geology and Palaeontology, University of Florence, own measurements), Pirro Nord and Dusino (University of Turin, own measurements), Senèze and Mugello (Guérin 1980), Chilhac (Boeuf 1995), Mundesley, Overstrand, Pakefield, Sidestrand, and Trimingham (Natural History Museum London, own measurements);
- *D. megarhinus* from Montpellier, Saint-Laurent-des-Arbres, Perpignan, and Lens-Lestang (Guérin 1980);
- *S. hemitoechus* from the Upper Travertines of Weimar Ehringsdorf (Senckenberg Research Station of Quaternary Palaeontology Weimar, Kahlke 1975, own measurements), Neumark-Nord (Van der Made 2010), Burgtonna (Kahlke 1978), Orvieto, Val di Chiana, Cava di Rena Capanelle, Arezzo (Museum of Geology and Paleontology, University of Florence, own measurements), Ilford, Grays, Clacton-on-Sea, West Thurrock (Natural History Museum London, own measurements), Binagady (Zoological Institute of the Russian Academy of Sciences St. Petersburg, own measurements), Steinheim, Swanscombe, Barrington, Peterborough, Minchin Hole, and Westerveld (Guérin 1980);
- *S. hemitoechus intermedius* from Mezzana Rabatone (Persico et al. 2015);
- *S. hemitoechus falconeri* from Bucine (Persico et al. 2015);
- *S. hemitoechus aretinus* from Botrio Maspino, Ponte alla Nave and San Colombano al Lambro (Persico et al. 2015);
- *S. kirchbergensis* from the Lower Travertine of Weimar Ehringsdorf and Taubach (Senckenberg Research Station of Quaternary Palaeontology Weimar, own measurements), Burgtonna (Kahlke 1978), Neumark-Nord (Van der Made 2010), Dechenhöhle (Lanser 1997), Gorzów Wielkopolski (Institute of Environmental Biology, University of Wrocław, own measurements), Siekierki (Museum of the Earth of the Polish Academy of Sciences Warsaw, own measurements), Spinadesco (Persico et al. 2015), Grays (Natural History Museum London, own measurements), Husnjakovo Brdo (Billia 2010), Chondon (Kirillova et al. 2017), Krasnyi Yar (Shpansky and Billia 2012), Irkutsk (Zoological Institute of the Russian Academy of Sciences St. Petersburg, own measurements), Russian Federation (Tomsk State University, own measurements), Mosbach, Krefeld, Steinheim, Ponte Galeria (Guérin 1980);

– *C. antiquitatis* from the Upper Travertines of Weimar-Ehringsdorf (Senckenberg Research Station of Quaternary Palaeontology Weimar, Kahlke 1975, own measurements), Neumark-Nord (Van der Made 2010), Pyskowice-Rzeczyce, Konin coalmine, Góra Puławska, Rzeszów Wistok near Lisia Góra and unknown localities (Museum of the Earth and Institute of Palaeobiology of the Polish Academy of Sciences Warsaw, own measurements), Creswell Crags (Museum of Palaeontology and Geology Bologna, own measurements), Emine-Bair-Khosar Cave (Emine-Bair-Khosar Museum at Mount Chatyr-Dag, Crimea, Ukraine, own measurements), Bukugański Quarry, Kaniv and unknown localities (Museum of Natural History of the Ukrainian Academy of Sciences Kiev, own measurements), Tomsk region (Tomsk State University, own measurements), Magadan, unknown localities in the Urals, Europe and Siberia, Yakutsk, Tobolsk (Museum of Natural History of the Ukrainian Academy of Sciences Kiev, Zoological Institute of the Russian Academy of Sciences, St. Petersburg, Museum of Geology and Palaeontology, University of Florence, Museum of Palaeontology and Geology Bologna, own measurements), Brengues, Jaurens, Lyon-l'Antiquaille, Saint-Germain-au-Mont-d'Or, La Fage, Coulon, Monte Circeo, Cambridge, Longstanton, Little Downham, Darmstadt, Gimbsheim, Kronberg, Lahde, Rehme, Mainz, Perivale Grange, London, Madrid, Gewande, Amsterdam, Rugby, Hofstade, Dendermonde, Lierre Dream Cave, Lawford, and Chesterton (Guérin 1980);
– *R. unicornis*, *R. sondaicus*, *D. sumatrensis*, *C. simum*, *D. bicornis* (Guérin 1980).

The Sumatran (*D. sumatrensis*) and Javan rhinoceroses (*R. sondaicus*) are the smallest of the five extant comparative species. *D. sumatrensis* reaches 100–150 cm in height at the withers and 600–950 kg in body weight. *R. sondaicus* has a height range of 150–170 cm and a body weight around 1,200–1,500 kg. In Asia, the body dimensions of both species are surpassed by the Indian rhinoceros (*R. unicornis*), which reaches 175–200cm in height and around 2,000kg in body mass. The African black rhinoceros (*D bicornis*) has dimensions of 140–170 cm and 800–1,300 kg and the white rhinoceros (*C. simum*) 150–180 cm and 1,350–3,500 kg (data from Dinerstein 2011).

When taking into account the dorsal length of the skull (**Fig. 2**, measurement 1; **Fig. 3**), the Untermassfeld specimen falls within the upper range of the dimensions recorded in the Italian *S. etruscus*, and within the lower range of *S. hundsheimensis* from various European sites. It is shorter than that recorded in *S. jeanvireti* from Vialette, as well as *D. megarhinus*, *S. hemitoechus*, *S. kirchbergensis,* and *C. antiquitatis* from various Eurasian sites. Compared with extant species, the dorsal length of IQW 2009/30 270 (Mei. 29 432) is longer than in the Javan and Sumatran rhinoceroses, falls within the upper ranges of the Indian and the black rhinoceros, and is significantly shorter than that of the skulls of the white rhinoceros.

At the widest point of its forehead (**Fig. 2**, measurement 17; **Fig. 3**), the Untermassfeld skull exceeds the ranges of *S. jeanvireti* from Vialette and various specimens of *S. etruscus* from Italy and Moldova. It falls within the range of *D. megarhinus*. It is broader than *S. hemitoechus intermedius* and *S. hemitoechus falconeri* from Italy and narrower than *S. hemitoechus aretinus* from Italy. The forehead width of the Untermassfeld skull is significantly narrower than those of *S. kirchbergensis,* with the exception of one specimen from Spinadesco. The widest point of the forehead of IQW 2009/30270 (Mei. 29432) is also smaller than that of woolly rhinoceroses from various Eurasian sites. Compared with extant species, the skull from Untermassfeld is wider than that of *R. sondaicus* and *D. sumatrensis,* falls within the upper range of *R. unicornis,* and in the lower ranges of *C. simum* and *D. bicornis*.

The relationship between the dorsal length and the widest point of the forehead determines the sculpture of the dorsal skull roof of a rhinoceros (**Fig. 3**). The total length of the skull, from the tip of the nasals to the caudal margin of the occipital condyles, is determined by the angle between the base of the skull and the occiput, which in turn reflects the posture of the animal's skull. The Sumatran and Javan rhinoceroses have the shortest dorsal cranial length, whereas the black and Indian rhinoceroses are just slightly longer dorsally These species are browsers and their occiputs are adjusted to this lifestyle. In the black rhinoceros

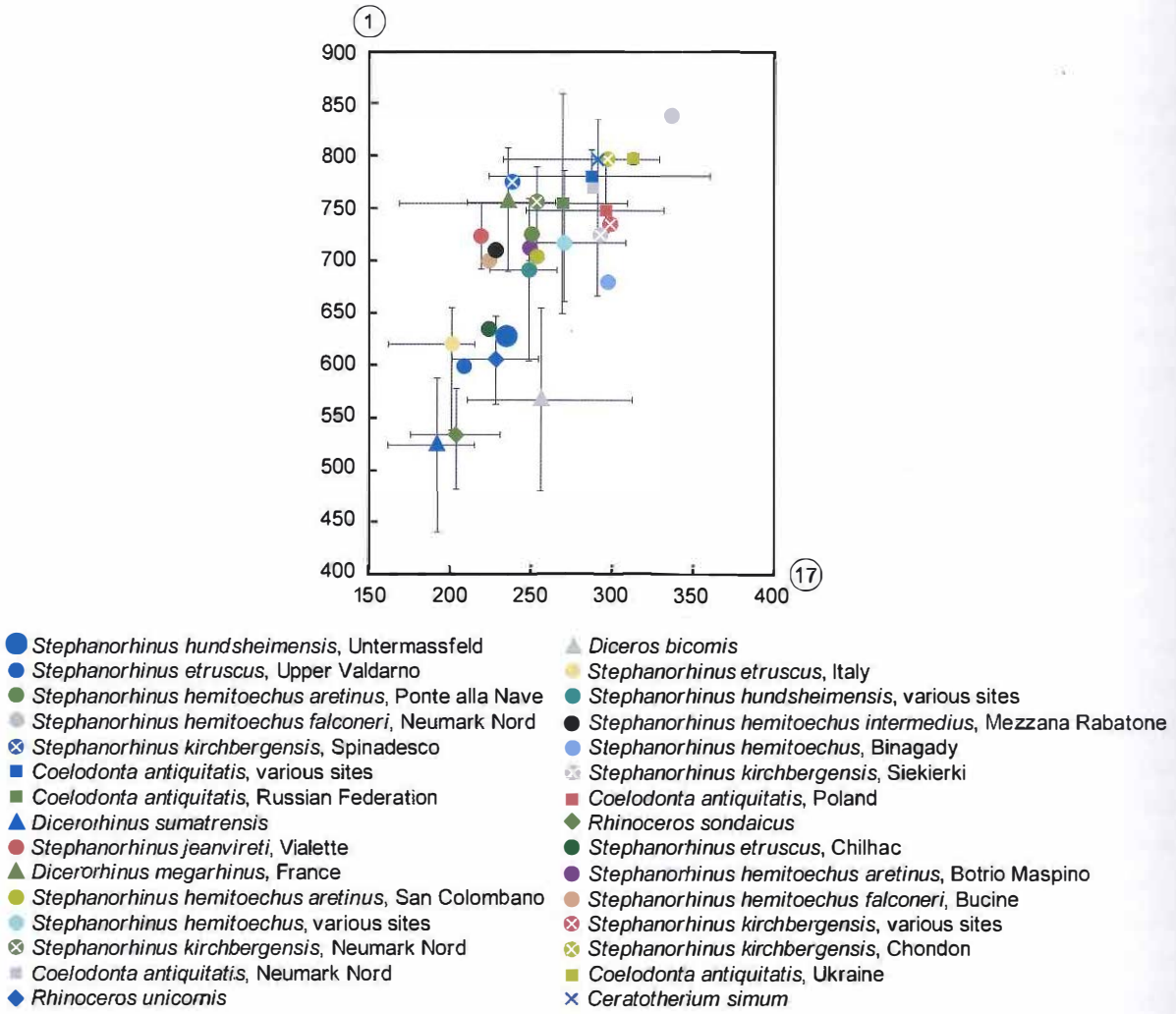

Fig. 3 Bivariate plot of dorsal length (1) versus the greatest width of the forehead (17).

the occiput forms an almost right angle to the base of the skull, whereas in the Indian rhinoceros it forms an acute angle. Despite its rather small body size (Ballatore 2016), *S. etruscus* had a skull of similar length but somewhat more slender in the orbital region; the long nasal bones of this species may explain the relatively long dorsal cranial length. The length of the Untermassfeld skull falls in the ranges of the longest skulls of the black and Indian rhinoceroses and of *S. etruscus*, but falls in the lower range of *S. hundsheimensis*. The largest comparative skulls considered here are those of *S. hemitoechus*, *S. kirchbergensis*, and of the woolly and white rhinoceroses.

Similar tendencies can be seen in the plot comparing the dorsal length to the total length of the skulls (**Fig. 2**, measurements 1 and 3; **Fig. 4**). The species considered for this study cluster into two groups. The first group includes the smaller species (*D. sumatrensis*, *S. etruscus*) along with the large browsers (*R. unicornis*, *D. bicornis*), whereas the second group consists of large-sized rhinoceroses with long nasals and backward-inclined occiputs (*S. hemitoechus*, *C. antiquitatis*, *C. simum*). This separation is evident when Indian rhinoceroses are compared with the woolly rhinoceroses from Russian sites. Both species are comparable in size, but use two different feeding strategies. They have similar mean dorsal lengths, but the skull of the Indian rhinoceros has a markedly smaller skull. IQW 2009/30270 (Mei. 29432) lies between at the boundary of the two main clusters and falls within the lower range of *S. hundsheimensis*.

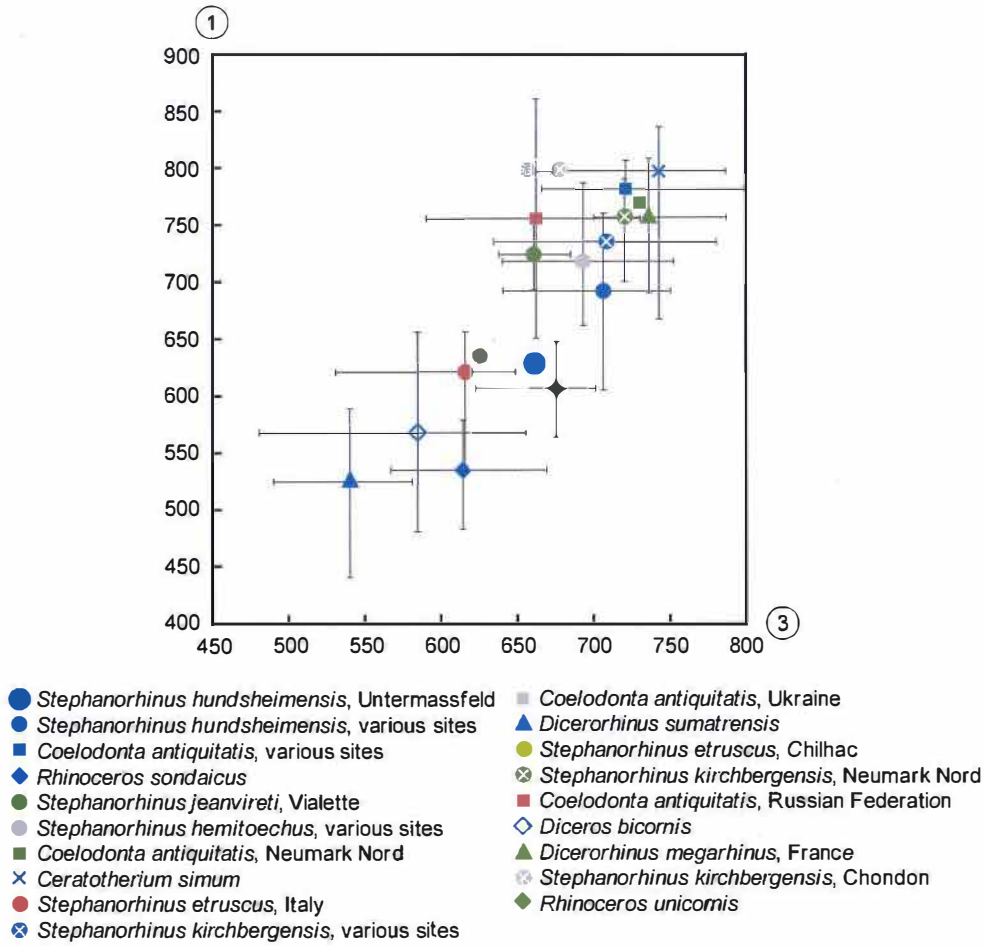

Fig. 4 Bivariate plot of dorsal length (1) versus total length of the skull (3).

The height of the occiput (**Fig. 2**, measurement 15; **Fig. 5**) of the Untermassfeld skull is either larger or falls within the upper range of the skulls of *S. etruscus* selected for this study. It fits within the variation of *S. hundsheimensis* from various European sites and is either smaller or included in the lower range of the dimensions of *S. kirchbergensis* and *C. antiquitatis*. Compared to the extant rhinoceroses, the occiput of the Untermassfeld skull is lower than those of the skulls of *R. unicornis*, *R. sondaicus*, and *C. simum*. In the Indian as well as in white rhinoceroses, the inclination of the occiput generates higher values. In the former it leans rostrally, whereas in the latter, caudally (see also Zeuner 1934). The height of the occiput in the Untermassfeld skull is close to the mean of *D. bicornis,* which has an occiput oriented similarly. Despite the deformation and damage of the Untermassfeld skull gives an inaccurate measurement (see section 2.), the narrow width of its occiput (**Fig. 2**, measurement 31; **Fig. 5**) is clearly noticeable. It falls within the ranges of *S. etruscus* and *D. sumatrensis* and is close to the minimum value of *D. bicornis*. In all the other species considered here the value is higher.

The relationship between the dorsal cranial lengths and the lengths from the tip of the nasals to the rostral margin of the orbit (**Fig. 2**, measurements 1 and 7; **Fig. 6**) separates the rhinoceros species used for this study into two major clusters. One includes *D. sumatrensis* and the species with perpendicular or rostrally leaning occiputs, i. e. *R. sondaicus*, *R. unicornis*, *D. bicornis*, and *S. etruscus*. The second consists

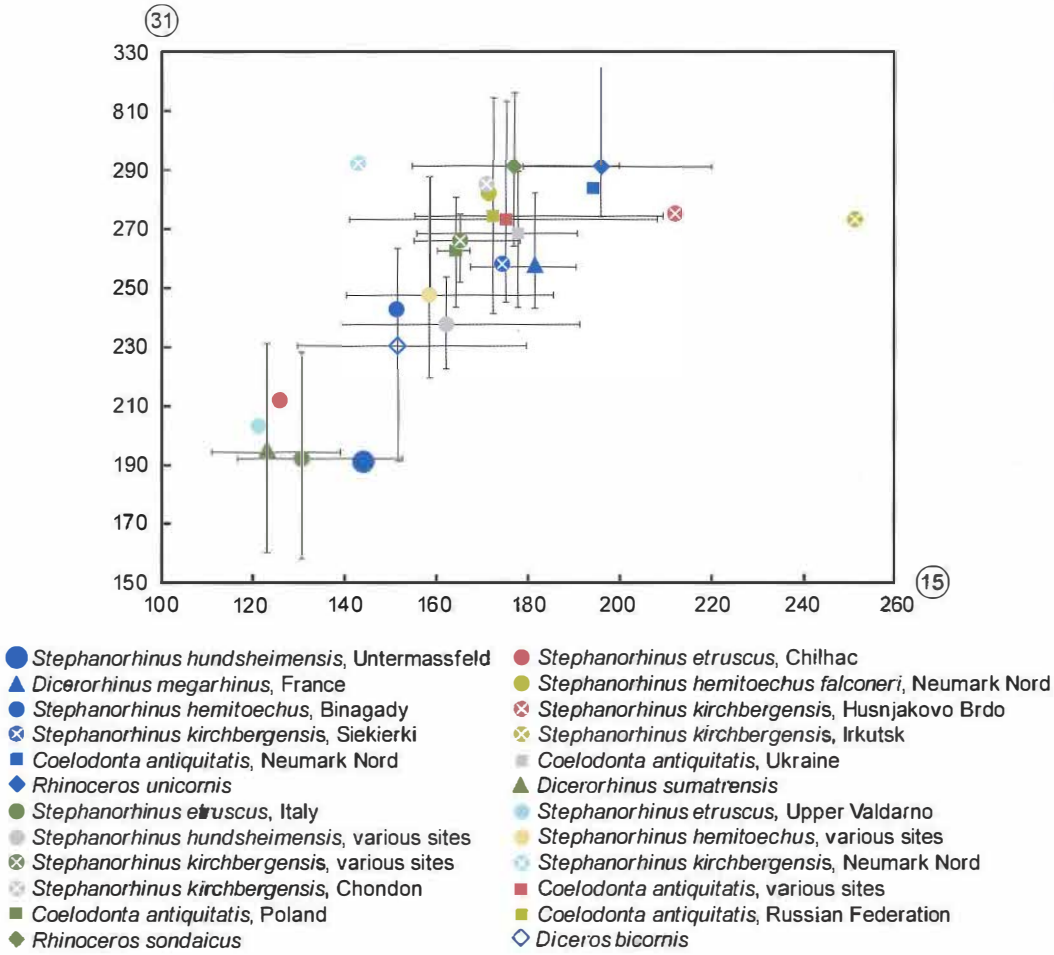

Fig. 5 Bivariate plot of the greatest width of the occiput (31) versus height of the squamous part of the occiput (15).

of dolichocephalic rhinoceroses, i. e. *C. simum, S. hemitoechus, C. antiquitatis*, and of large-sized rhinoceroses with less elongated skulls, namely *D. megarhinus, S. jeanvireti, S. hundsheimensis*, and *S. kirchbergensis*. The Untermassfeld specimen falls between the two clusters and is therefore an intermediate representative.

The distance between the nasoincisive notch and the rostral margin of the orbit (**Fig. 2**, measurement 6; **Fig. 7**) can be considered as the combined lengths of the maxillary, lacrimal and zygomatic bones, which form a buttress for the massive frontal part of the skull. In the Untermassfeld skull this section is more gracile than in *S. jeanvireti, D. megarhinus, C. antiquitatis, R. unicornis, C. simum,* and *D. bicornis*. It fits closer to the variation observed in *S. etruscus* and *S. hundsheimensis* and is positioned in the lowermost range of *S. hemitoechus, S. kirchbergensis,* and *R. sondaicus*.

The distance between the tip of the nasals and the nasoincisive notch (**Fig. 2**, measurement 5; **Fig. 7**) represents the length of the nose. The Untermassfeld specimen has a higher value than that observed in *S. jeanvireti* and all of the extant species. It lies below the mean of *D. megarhinus* and the European *S. hundsheimensis* used for the present study, but close to the mean of various representatives of *S. kirchbergensis*. It falls within, or even exceeds, the range recorded from samples of woolly rhinoceroses.

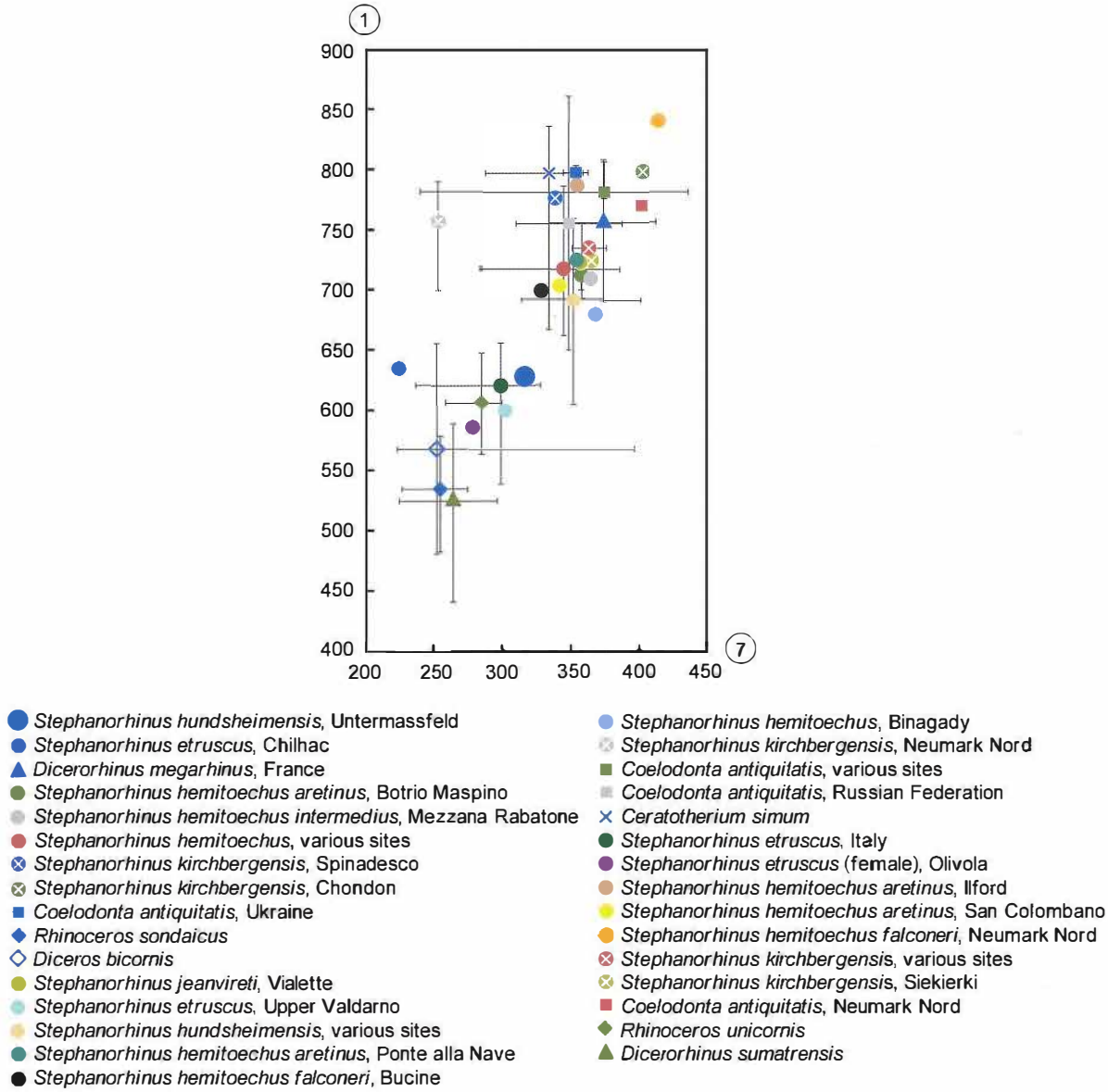

Fig. 6 Bivariate plot of the dorsal length (1) versus the distance from the tip of the nasals to the rostral margin of the orbit (7).

The middle part of the skull (measurement 6) supports a substantial part of the mass of the horns. Measurement 5 (**Fig. 2**) is the length of the nasals and thus the length of the lever carrying the mass of the nasal horn. The relationship between these two parameters (**Fig. 7**) divides the rhinoceroses considered here into several groups, reflecting the different dimensions of their horns.

Two are single-species groups. The first includes *D. bicornis*, which has the shortest nasals. This species develops large and heavy horns of up to 130 cm (anterior) and 55 cm (posterior) in length. Due to its short nose the weight of the horns rests on the maxilla. The second single-species group includes the white rhinoceros, *C. simum*, yet another rhinoceros with large and heavy horns up to 102 cm (anterior) and 55 cm (posterior) long (data from Dinerstein 2011). Its nasals as well as the distance between the narial notch and the rostral margin of the orbit are longer than in *D. bicornis*, which offers stronger support for the mass of the horns.

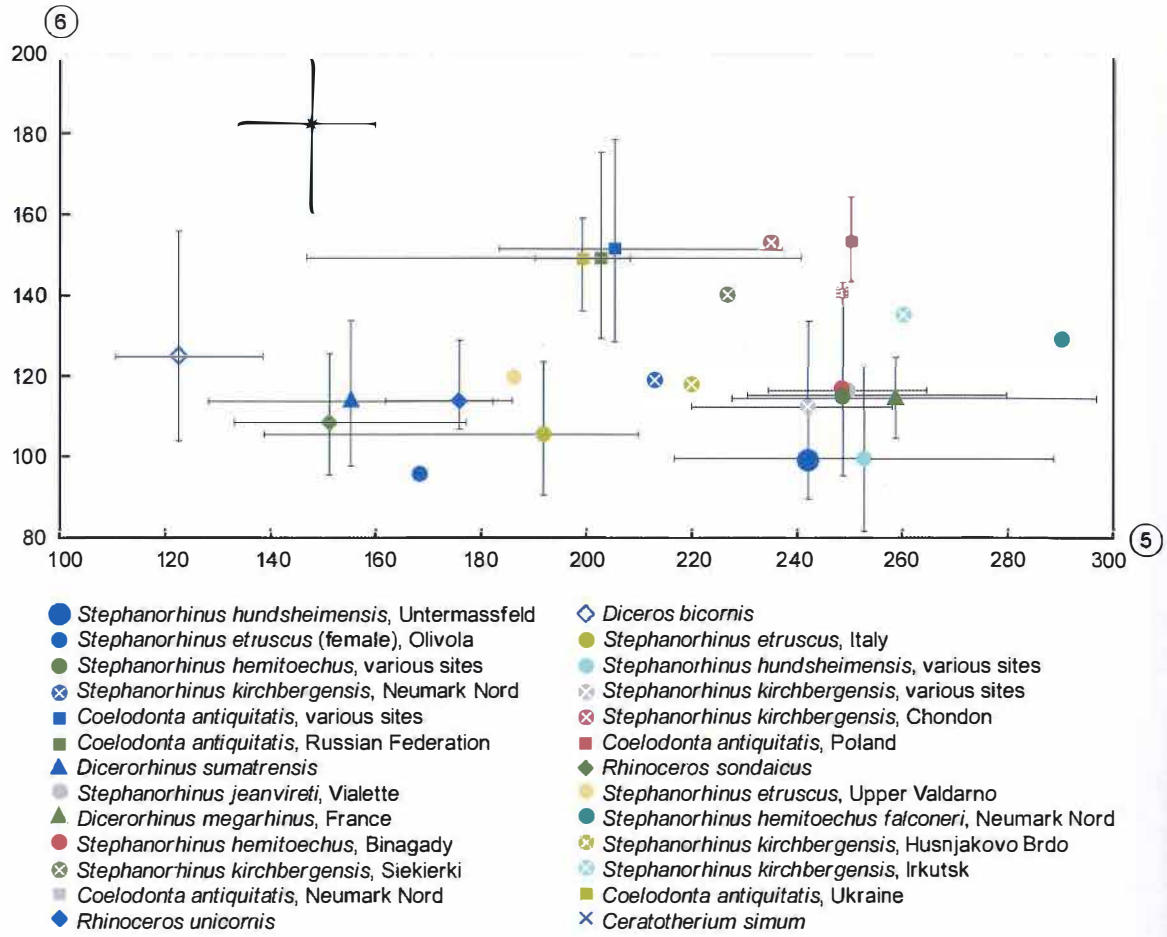

Fig. 7 Bivariate plot of the distance from the caudal-most point of the nasoincisive notch to the rostral border of the orbit (6) versus the distance from the tip of the nasals to the caudal-most point of the nasoincisive notch (5).

A further group consists of extant Asian rhinoceroses and *S. etruscus*. Both Indian and Javan rhinoceroses are relatively small single-horned species. In both horn lengths average around 25 cm. Javan rhinoceroses include hornless females (Dinerstein 2011). Sumatran rhinoceroses are two-horned and are generally the smallest of all extant rhinoceroses. Although certain museum specimens are known to have horns reaching 25–80cm, these should not be treated as average indicators (Dinerstein 2011). Extant short-horned Asian species have long nasals overhanging relatively gracile maxilla. In this group the tandem-horned *S. etruscus* has the longest nasals; an incipient ossification of the nasal septum warrants an additional support to the tip of the nasals.

Another group in **Fig. 7** comprises *S. jeanvireti*, *D. megarhinus*, *S. hundsheimensis*, *S. hemitoechus*, and *S. kirchbergensis*, all two-horned rhinoceroses with the longest distances between the nasoincisive notch and the orbit (**Fig. 2**, measurement 6). The shortest value, i.e. the most gracile middle part of the skull, is recorded in *S. hundsheimensis*, which in fact has the lowest horn mass of the whole group. The skull from Untermassfeld fits the range of *S. hundsheimensis*, consistently with the very delicate rugosity of its horn bases, and therefore the small size of its horns in life. Measurement 6 reaches the highest values in the other species of this group, indicating that *S. kirchbergensis* and *S. hemitoechus* probably had horns of significant size and massiveness, comparable with those of extant black rhinoceroses.

Quite expectedly, *C. antiquitatis* forms a cluster of its own. In this case the length of the nasals (**Fig. 2**, measurement 5) falls between the values recorded for extant rhinoceroses and for species from the previously

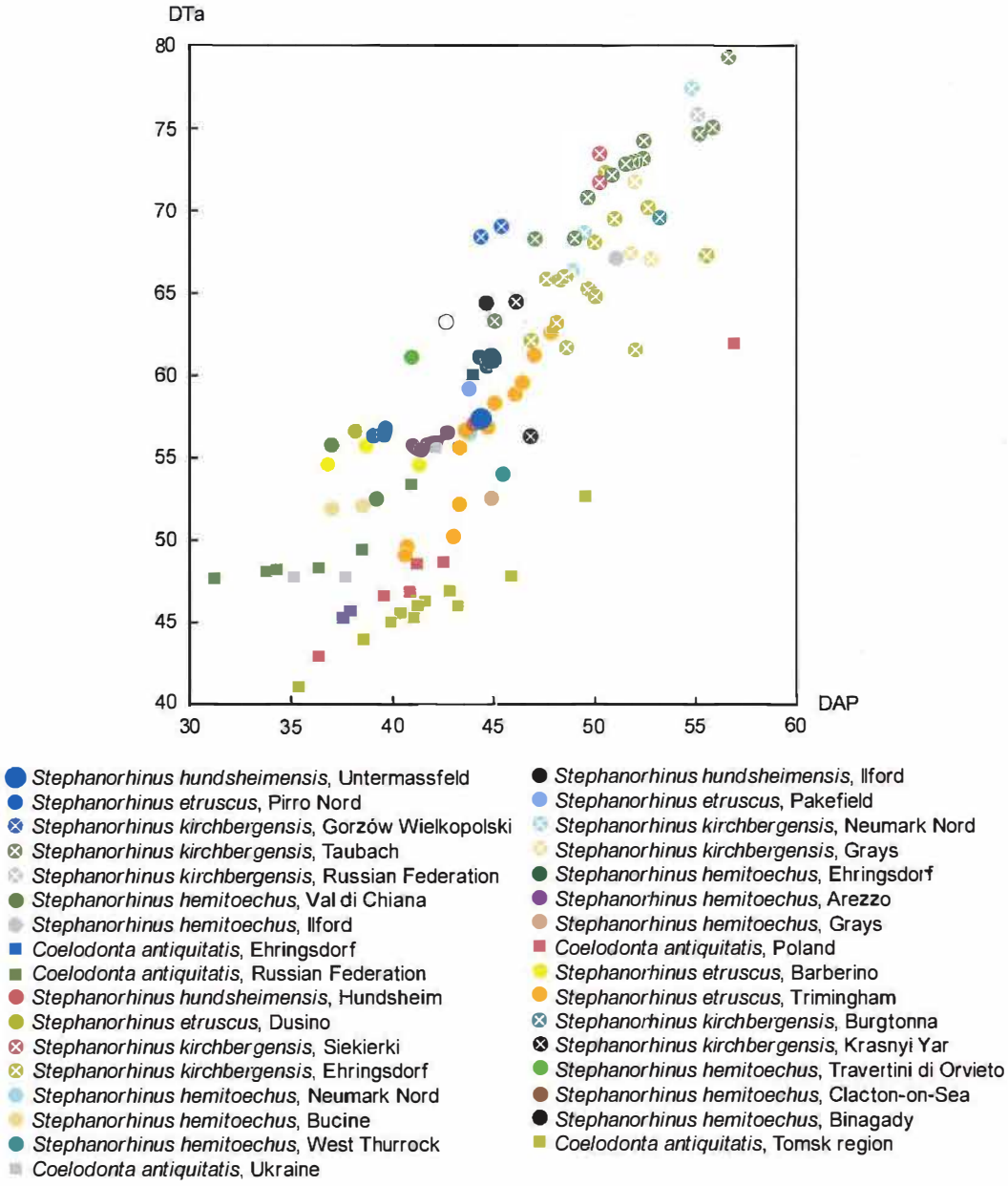

Fig. 8 Bivariate plot of the widest anterior transverse part of the crown (DTa) versus the antero-posterior buccal length (DAP) of the P^4.

described group of *S. jeanvireti*, *D. megarhinus*, *S. hundsheimensis*, *S. hemitoechus*, and *S. kirchbergensis*. The skulls of the woolly rhinoceros have long narial notch – orbit distances (**Fig. 2**, measurement 6). Nasal horns of *C. antiquitatis* from the permafrost can reach lengths of up to 132 cm (Garutt 1998). The downward-bent anterior portion of the nasals in woolly rhinoceroses indicates that the nasal horn clearly inclined forward. This indicates that the anterior horn had a regular and alternating contact with the ground, as confirmed, particularly in older individuals, by wear surfaces with distinct left and right facets (discussion in Kahlke 1999, 90). It is quite likely that advanced woolly rhinoceroses often carried their anterior horn nearly parallel to the ground, in order to shift the strain to the frontal part of the nasals, thereby inducing changes in the skull morphology that are exclusive to this species.

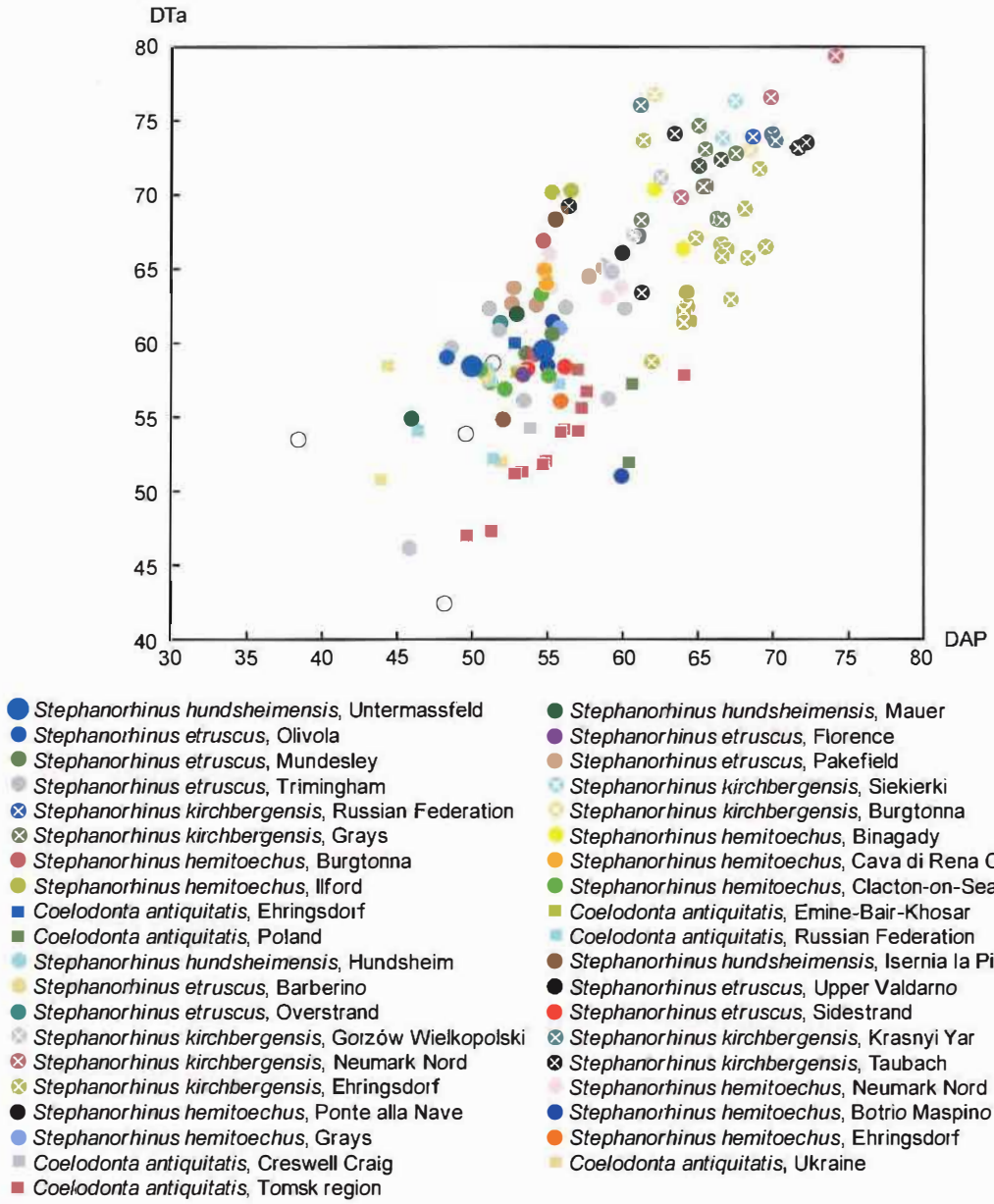

Fig. 9 Bivariate plot of the widest anterior transverse part of the crown (DTa) versus the antero-posterior buccal length (DAP) of the M^2.

In terms of tooth sizes, *S. kirchbergensis* has the largest P^4 and woolly rhinoceroses the smallest. The P^4 of the Untermassfeld skull are near to the range of *S. etruscus*, *S. hundsheimensis* and *S. hemitoechus* (**Fig. 8**). A similar tendency is visible in the M^2 (**Fig. 9**).

The morphometric traits discussed here confirm the assignment of the described rhinoceros skull from Untermassfeld to the species *Stephanorhinus hundsheimensis* (see section 1.). The measured dimensions are generally lower than the mean values for this species. Morphologically and dimensionally, IQW 2009/30 270 (Mei. 29432) is an adult female individual with a pair of very small horns.

S. hundsheimensis was widespread in the western Palaearctic from the late Early to the early Middle Pleistocene, i.e. approximately between 1.4 and 0.5 Ma BP (Fortelius et al. 1993; Mazza et al. 1993; Lacombat 2005; Schreiber 2005; Kahlke et al. 2011). Ecologically, it was the most tolerant rhinoceros species of

the Palaearctic Plio-Pleistocene, with a dietary variability ranging from pronounced grazing to dominantly browsing regimes (Kahlke and Kaiser 2011)

5. Conclusions

Surprisingly, the very rich rhinocerotid material from Untermassfeld includes only one almost complete skull of an adult individual. *Pachycrocuta brevirostris* fed heavily on the carcass, leaving evident damage on the occiput and left side of the specimen. At some point, and most probably at the latest during transportation by flowing water, both keratin horns became separated from the head. Elements that tend to resist water transport and remain behind forming lag deposits are underrepresented or even lacking in the Untermassfeld fossil assemblage. The horns of the rhinoceros carcass would have increased the resistance to the free movement of the skull. The capsized position of the isolated skull suggests that the horns had likely been removed from it somehow and sometime prior to its transportation to the area of the site by streaming water. Just after the peak of a powerful riverine flood event, the isolated cranium was embedded in an erosion channel immediately leeside of a clastic mudflow fan, becoming part of a large, dense mammal bone accumulation. The fossil was then subjected to carbonate impregnation and plastic deformation, which are the typical general pattern of diagenetic processes at the site of Untermassfeld.

The morphological traits and dimensions of the Untermassfeld skull confirm its assignment to *Stephanorhinus hundsheimensis*, although it is the smallest of the skulls of this species analysed for this study. In addition to the individual size and the narrow, gracile construction of the nasal region, the reduced rugosity of both horn bases suggests that the specimen belonged to a female individual. The Untermassfeld specimen probably had the smallest pair of horns of all the Pleistocene and extant rhinoceroses examined for this study.

By comparing the ratios of the nasal length to the distance between the narial notch and the rostral rim of the orbit we come up with five types of patterns evolved by the various species studied here to support the weight of the horns. The discrimination becomes even more evident when the degree of ossification of the nasal septum is considered. *S. hundsheimensis* groups up with *S. hemitoechus* and *S. kirchbergensis*, although the horns of the former were perhaps somewhat lighter, as indicated by the smaller average distance between the nasal aperture and the orbit than in the latter two species.

The rhinocerotid palaeo-population from Untermassfeld belongs to the older representatives of *S. hundsheimensis* in the western Palaearctic (Lacombat 2006a). The Hundsheim rhinoceros is one of the key mammal species of the Epivillafranchian biochron (Kahlke 2007b).

Acknowledgements

We thank D. Rössler (Weimar) for the preparation of the described rhinoceros skull and particularly for the repeated turning of the heavy and very fragile specimen using various specially made auxiliary staffages. Our thanks go to T. Korn (Weimar) for the photographs used in this chapter. A. K. and K. S. wish to thank the curators of the visited palaeontological collections, especially G.F. Baryshnikov (Saint Petersburg), E. Cioppi (Florence), U.T. Hohenstein (Ferrara), G. Jakubowski (Warsaw), M. Komar (Kiev), A. Kozlov (Emine-Bair-Khosar), S. Pappa (London), M. Pavia (Turin), C. Sarti (Bologna) and A.V. Shpansky (Tomsk), for their hospitality and friendly support during the comparative work. We are grateful to E. Haase (Weimar) for compiling the illustrations and especially for her patience in the final production of the diagrams. J. Arnold (Weimar) upda-

ted the NISP and MNI of the Untermassfeld rhinoceros finds and C. Nielsen-Marsh (Leipzig) kindly edited the English text. P.P.A. Mazza (Florence) supported our study with critical comments and important information

References

Ballatore, M., 2016. Palaeoecological investigations on Plio-Pleistocene European rhinoceroses (genus *Stephanorhinus*): powder x-ray diffraction, carbon isotope geochemistry, tooth wear analyses and biometry. Plinius [online] 42, 16–19. Available: https://doi.org/10.19276/plinius.2016.01001. [Accessed 08 July 2019]

Billia, E.M.E., 2010. The famous *Stephanorhinus kirchbergensis* (Jäger, 1839) »Irkutsk skull« (Mammalia, Rhinocerotidae) from Eastern Siberia briefly compared with those from Krapina and Warsaw (Eastern Europe). In: Proceedings of the International Scientific Conference »The Museum and the Scientific Research« (Craiova, Romania, September 16–18, 2010). Oltenia. Studii şi comunicări. Ştiinţele Naturii 26, 296–302.

Boeuf, O., 1995. Le *Dicerorhinus etruscus* (Rhinoceretidae, Mammalia) du site pliocène supérieur de Chilhac (Haute-Loire, France). Geobios 28, 383–391.

Dinerstein, E., 2011. Family Rhinocerotidae (Rhinoceroses). In: Wilson, D.E., Mittermeier, R.A. (Eds.), Handbook of the Mammals of the World. Volume 2: Hoofed Mammals. Barcelona, 144–181.

Ellenberg, J., Kahlke, R.-D., 1997. Die quartärgeologische Entwicklung des mittleren Werratals und der Bau der unterpleistozänen Komplexfundstelle Untermaßfeld. In: Kahlke, R.-D. (Ed.), Das Pleistozän von Untermaßfeld bei Meiningen (Thüringen). Teil 1. Monographien des Römisch-Germanischen Zentralmuseums 40, 1, 29–62, pls. 1–18.

Fortelius, M., Mazza, P., Sala, B., 1993. *Stephanorhinus* (Mammalia: Rhinocerotidae) of the western European Pleistocene, with a revision of *S. etruscus* (Falconer, 1868). Palaeontographia Italica 80, 63–155.

Garutt, N., 1998. Neue Angaben über die Hörner des Fellnashorns *Coelodonta antiquitatis*. Deinsea 4, 25–40.

Guérin, C., 1980. Les rhinocéros (Mammalia, Perissodactyla) du Miocène terminal au Pléistocène supérieur en Europe occidentale. Comparaison avec les espèces actuelles. Documents du Laboratoire de Geologie de la Faculte des Sciences de Lyon 79, 2, 423–783.

Kahlke, H.D., 1972. Die Rhinocerotiden-Reste der Stránská Skála bei Brno. In: R. Musil (Ed.), Stránská Skála I. 1910 -1945, Anthropos 20, nova seria 12, 175–176

1975. Die Rhinocerotiden-Reste aus den Travertinen von Weimar-Ehringsdorf. Abhandlungen des Zentralen Geologischen Instituts, Paläontologische Abhandlungen 23, 337–397, pls. XXVII–XXXII, 1 map.

1978. Die Rhinocerotiden-Reste aus den Travertinen von Burgtonna in Thüringen. Quartärpaläontologie 3, 129–135, pls. 34–37.

1980. Flußpferde an der Werra. In: Urania-Universum 26. Leipzig, Jena, Berlin, 495–500.

1982. *Hippopotamus antiquus* Desmarest, 1822 aus dem Pleistozän von Meiningen in Südthüringen (Bezirk Suhl). Zeitschrift für geologische Wissenschaften 10, 943–949

2001. Die Rhinocerotiden-Reste aus dem Unterpleistozän von Untermaßfeld. In: Kahlke, R.-D. (Ed.), Das Pleistozän von Untermaßfeld bei Meiningen (Thüringen). Teil 2. Monographien des Römisch-Germanischen Zentralmuseums 40, 2, 501–555, pls. 79–91.

Kahlke, R.-D., 1997. Zur Entdeckungs- und Erforschungsgeschichte der unterpleistozänen Komplexfundstelle Untermaßfeld. In: Kahlke, R.-D. (Ed.), Das Pleistozän von Untermaßfeld bei Meiningen (Thüringen). Teil 1. Monographien des Römisch-Germanischen Zentralmuseums 40, 1, 1–28.

1999. The History of the Origin, Evolution and Dispersal of the Late Pleistocene *Mammuthus-Coleodonta* Faunal Complex in Eurasia (Large Mammals). Rapid City, SD.

2001. Die unterpleistozäne Komplexfundstelle Untermaßfeld – Zusammenfassung des Kenntnisstandes sowie synthetische Betrachtungen zu Genesemodell, Paläoökologie und Stratigraphie. In: Kahlke, R.-D. (Ed.), Das Pleistozän von Untermaßfeld bei Meiningen (Thüringen). Teil 3. Monographien des Römisch-Germanischen Zentralmuseums 40, 3, 931–1030, suppl. 1–15.

2006. Untermassfeld. A late Early Pleistocene (Epivillafranchian) fossil site near Meiningen (Thuringia, Germany) and its position in the development of the European mammal fauna. British Archaeological Reports, International Series 1578. Oxford.

2007a. Bericht zu den bodendenkmalpflegerischen Maßnahmen an der unterpleistozänen Komplexfundstelle Untermaßfeld im Jahr 2007. Unpublished excavation report. Weimar

2007b. Late Early Pleistocene European large mammals and the concept on an Epivillafranchian biochron. In: Kahlke, R.-D., Maul, L.C., Mazza, P.P.A. (Eds.), Late Neogene and Quaternary biodiversity and evolution: Regional developments and interregional correlations. Proceedings of the 18th International Senckenberg Conference (VI International Palaeontological Colloquium in Weimar), Vol. II. Courier Forschungsinstitut Senckenberg 259, 265–278.

in volume 5. The Pleistocene of Untermassfeld – Synopsis on site formation, faunal assemblage, palaeoenvironment, biostratigraphy and position in the western Palaearctic faunal history. In: Kahlke, R.-D. (Ed.), The Pleistocene of Untermassfeld near Meiningen (Thüringen, Germany). Part 5. Monographien des Römisch-Germanischen Zentralmuseums 40, 5.

Kahlke, R.-D., Kaiser, T.M., 2011. Generalism as a subsistence strategy: advantages and limitations of the highly flexible feeding traits of Pleistocene *Stephanorhinus hundsheimensis* (Rhinocerotidae, Mammalia). Quaternary Science Reviews 30, 2250–2261.

Kahlke, R.-D., Linnemann, U., Gärtner, A., in this volume. New results on the origin and geological history of the Early Pleistocene site of Untermassfeld. 1079–1104.

Kahlke, R.-D., García, N., Kostopoulos, D.S., Lacombat, F, Lister, A.M., Mazza, P.P.A., Spassov, N., Titov, V.V., 2011. Western Palaearctic palaeoenvironmental conditions during the Early and early Middle Pleistocene inferred from large mammal communities, and implications for hominin dispersal in Europe. Quaternary Science Reviews 30, 1368–1395.

Kirillova, I.V., Chernova, O.F, Van der Made, J., Kukarskih, V.V., Shapiro, B., Van der Plicht, J., Shidlovskiy, F.K., Heintzman, P.D., Kolfschoten, T.v., Zanina, O.G., 2017. Discovery of the skull of *Stephanorhinus kirchbergensis* (Jäger, 1839) above the Arctic Circle. Quaternary Research 80, 537–550.

Kretzoi, M., 1942. Bemerkungen zum System der nachmiozänen Nashorn-Gattungen. Földtani Közlöny 72, 309–318.

Lacombat, F., 2005. Les rhinocéros fossiles des sites préhistoriques de l'Europe méditerranéenne et du Massif Central. Paléontologie et implications biochronologiques. British Archaeological Reports, International Series 1419. Oxford.

2006a. Pleistocene Rhinoceroses in Mediterranean Europe and in Massif Central (France). In: Kahlke, R.-D., Maul, L.C., Mazza, P.P.A. (Eds.), Late Neogene and Quaternary biodiversity and evolution: Regional developments and interregional correlations. Proceedings of the 18th International Senckenberg Conference (VI International Palaeontological Colloquium in Weimar), Vol. I. Courier Forschungsinstitut Senckenberg 256, 57–69.

2006b. Morphological and biometrical differentiation of the teeth from Pleistocene species of *Stephanorhinus* (Mammalia, Perissodactyla, Rhinocerotidae) in Mediterranean Europe and the Massif Central, France. Palaeontographica, Abteilung A 274, 71–111.

2007. Phylogeny of genus *Stephanorhinus* in the Plio-Pleistocene of Europe. Hallesches Jahrbuch für Geowissenschaften 23, 63–64.

Lanser, K-P, 1997. Der Schädel eines dicerorhinen Nashorns aus der Dechenhöhle bei Iserlohn-Letmathe. Geologie und Paläontologie in Westfalen 47, 53–78.

Mazza, P, Sala, B., Fortelius, M., 1993. A small latest Villafranchian (late Early Pleistocene) rhinoceros from Pietrafitta (Perugia, Umbria, Central Italy), with notes on the Pirro and Westerhoven rhinoceroses. Paleontographia Italica 80, 25–50.

Persico, D., Billia, E.M.E., Ravara, S., Sala, B., 2015. The skull of *Stephanorhinus kirchbergensis* (Jäger, 1839) (Mammalia, Rhinocerotidae) from Spinadesco (Cremona, Lombardia, Northern Italy): morphological analyses and taxonomical remarks – an opportunity for revising the three other skulls from the Po Valley. Quaternary Science Reviews 109, 28–37.

Schreiber, H.D., 1999. Untersuchungen zur Variabilität von *Stephanorhinus hundsheimensis* (Toula, 1902) und der Nachweis von *S. kirchbergensis* (Jäger, 1839) an Skelettmaterial aus dem Mittelpleistozän von Mauer bei Heidelberg (SW-Deutschland). Diploma thesis, Rheinische Friedrich-Wilhelms-Universität zu Bonn, Germany

2005. Osteological investigations on skeleton material of rhinoceroses (Rhinocerotidae, Mammalia) from the early Middle Pleistocene locality of Mauer near Heidelberg (SW-Germany). In: Crégut-Bonnoure, É. (Ed.), Les Ongulés Holarctiques du Pliocène et du Pléistocène. Quaternaire, hors-série 2, 103–111.

Shpansky, A.V., Billia, E.M.E., 2012. Records of *Stephanorhinus kirchbergensis* (Jäger, 1839) (Mammalia, Rhinocerotidae) from the Ob' River at Krasny Yar (Tomsk region, southeast of Western Siberia). Russian Journal of Theriology 11, 47–55.

Toula, F., 1902. Das Nashorn von Hundsheim. *Rhinoceros* (*Ceratorhinus* Osborn) *hundsheimensis* nov. form. Abhandlungen der Kaiserlich-Königlichen Geologischen Reichsanstalt 19, 1–92.

Van der Made, J., 2010. The rhinos from the Middle Pleistocene of Neumark-Nord (Saxony-Anhalt). In: Mania, D. et al., Neumark-Nord – Ein interglaziales Ökosystem des mittelpaläolithischen Menschen. Veröffentlichungen des Landesamtes für Denkmalpflege und Archäologie Sachsen-Anhalt – Landesmuseum für Vorgeschichte 62, 433–527.

Wagner, M.-T., 2008a. Aus der Eiszeit in die Zukunft. Welt-Wissen vom Werra-Strand. Die eine Million Jahre lange Geschichte eines Thüringer Tieres. Teil 1. Südthüringer Zeitung 17. April 2008, Schmalkalden.

2008b. Mit Zahnarztinstrumenten auf Schatzsuche. Welt-Wissen vom Werra-Strand. Die eine Million Jahre lange Geschichte eines Thüringer Tieres. Teil 2. Südthüringer Zeitung 23. April 2008, Schmalkalden.

2008c. »Es ist ein Mädchen« – aus der Eiszeit. Welt-Wissen vom Werra-Strand. Die eine Million Jahre lange Geschichte eines Thüringer Tieres. Teil 3. Südthüringer Zeitung 30. April 2008, Schmalkalden.

Zeuner, F, 1934. Die Beziehungen zwischen Schädelform und Lebensweise bei den rezenten und fossilen Nashörnern. Berichte der Naturforschenden Gesellschaft zu Freiburg i. Br 34, 21–80.